Review

Discharge Estimation over Piano Key Weirs: A Review of Recent Developments

Raj Kumar Bhukya [1], Manish Pandey [1,*], Manousos Valyrakis [2,*] and Panagiotis Michalis [3,4]

1. Department of Civil Engineering, National Institute of Technology Warangal, Warangal 506004, Telangana, India
2. Water Engineering Laboratory, School of Engineering, University of Glasgow, Glasgow G12 8LT, UK
3. School of Civil Engineering, National Technical University of Athens, 15773 Athens, Greece
4. Research and Innovation Department, INNOVATEQUE, 15561 Athens, Greece
* Correspondence: mpandey@nitw.ac.in (M.P.); manousos.valyrakis@glasgow.ac.uk (M.V.)

Abstract: The piano key (PK) weir has advanced over the labyrinth weir to increase the discharge capacity. Piano key weirs exhibit nonlinear flow behavior and are easy to place on the existing spillway or newly constructed dam with less base area. Various investigators are given equations to calculate the discharge coefficient for free and submerged flow conditions. The study focuses on reviewing the impacts of the PK weir geometry on the weir flow discharge coefficient, including weir length and height, upstream and downstream key widths, and apex overhangs. In this study, all possible aspects of PK weirs were briefly reviewed. From sensitivity analysis, it is observed that the discharge coefficient of the PK weir is more sensitive for the *L/W* dimensionless ratio followed by the *B/P* ratio. *L* is total length of the weir crest, *W* is width of the weir, *B* is total width of PK weir and *P* is height of the weir. This review paper is intended to serve as an accessible resource for hydraulic structures researchers and hydraulic engineering professionals alike interested in the hydraulics of PK weirs.

Keywords: piano key weirs; conventional labyrinth weir; discharge coefficient; flow-through hydraulic structures; hydraulics

1. Introduction

Piano key weir (PK weir) is a recently developed type of hydraulic infrastructure aiming to increase the discharge of an existing dam in spillway hydraulics to release more discharge and improve the performance by reducing the construction cost. This is of significant importance, taking into account the growing number of ageing dams, the increase in intensity and frequency of extreme climatic events [1], and the highly disruptive failure events and cascading incidents on critical infrastructure systems [1].

PK weirs are the improvements over the labyrinth weir developed by Hydro coop (France) in collaboration with the laboratory of hydraulic development of the University of Briska (Algeria). The national laboratory of hydraulic and environment of Electricite de France (EDF) and first model indicates the discharge increased by 4 to 5 times by replacing the PK weir [1]. More than 25 PK weirs are now in operation or under construction worldwide. The modified labyrinth weir length is more compared to the straight linear weir. The top view of the labyrinth weir is triangular or zig-zag, and the top view of the PK weir is rectangular. These rectangular keys guide the flow into inlet keys. PK weirs are important to increase the discharge capacity of the existing system, though it can play a key role on dissipating flood stress of reservoirs. PK weirs have more advantages over a labyrinth weir [1]. Due to its complexity in shape, there is no universal design for safe and economical design.

The discharge coefficient (C_D) of a weir is important because it deals with the overflow capacity of the dam to be safe against structural failure. Initial flow rate through the opening

can be predictable with the weir equation with corresponding coefficient of discharge because the water volume controlled by a dam can be considered as static. However, in case of a structural failure, flow characteristics from the opening are more complex. The PK weir geometrical parameters are: P is weir height, inlet key, and outlet key; widths are Wi, and Wo and the channel width is W; and the inlet key and outlet key lengths are Bi and Bo, respectively shown in Figure 1 and Table 1. The PK weir is constructed with sloped floors and overhangs, easy availability of construction materials, and less footprint area is required to construct it on top of existing or new dams, which are major advantages over a labyrinth weir. Increasing the crest length depends upon the cost of the spillway and location. Extended crest length is formed due to folding weir into compact 3D weir shapes, such as: arced, duck bull, minimum energy loss (MEL) weirs; box-inlet drop spillways; and labyrinth weirs [2–6]. PK weirs are used with gravity dams and natural channels [7–12] and can replace any affected gated spillways to increase the performance of operations and maintenance [13–15]. The first PK weir was put into operation in France in 2006 [15]. Anderson and Tullis [16] performed an experimental study to compare the CD of the PK weir with the traditional labyrinth weir and concluded that the labyrinth weir is the least hydraulic efficient. Ribeiro et al. [17] compared the CD for normal crested and sharp-crested PK weirs and concluded that PK weirs with sharp-crests gave more discharge for low water heads. Types A, B, C, and D of PK weirs are the overhanging of keys on both sides, only overhang on the upstream side, only overhang on the downstream side, and no overhanging on both sides, respectively (as can be seen in Figures 1–3). Kabiri-Samani and Javaheri [18] conducted an experimental study for type A, B, C, and D PK weirs. The author proposed a mathematical expression for calculating CD applicable to all PK weirs viz. type A, B, C, and D for free and submerged flow conditions. Machiels et al. [19] conducted an experimental study on PK weir discharge with and without parapet wall and concluded that by reducing the bottom slope with the weir height kept constant, the weir discharge increased.

Table 1. Geometrical parameters of PK weir.

| Parameter	Definition
B	Upstream–downstream key length, $B = B_o + B_b + B_i$
B_b	Sidewall length between inlet and outlet key crest axis
B_i, B_o	Inlet, outlet key length
H	Head over the weir crest on the upstream side of the weir
H_T	Total head on the upstream side of the weir
H_{TD}	Total head on the downstream side of the weir
L	Total developed length of the overflow crest axis
P	PK weir height
P_i, P_o	Height of the inlet key and outlet key entrance
S_i, S_o	The slope of inlet and outlet key
T_s	Sidewall thickness
W	Total width of the PK weir
W_i, W_o	Width of inlet and outlet keys
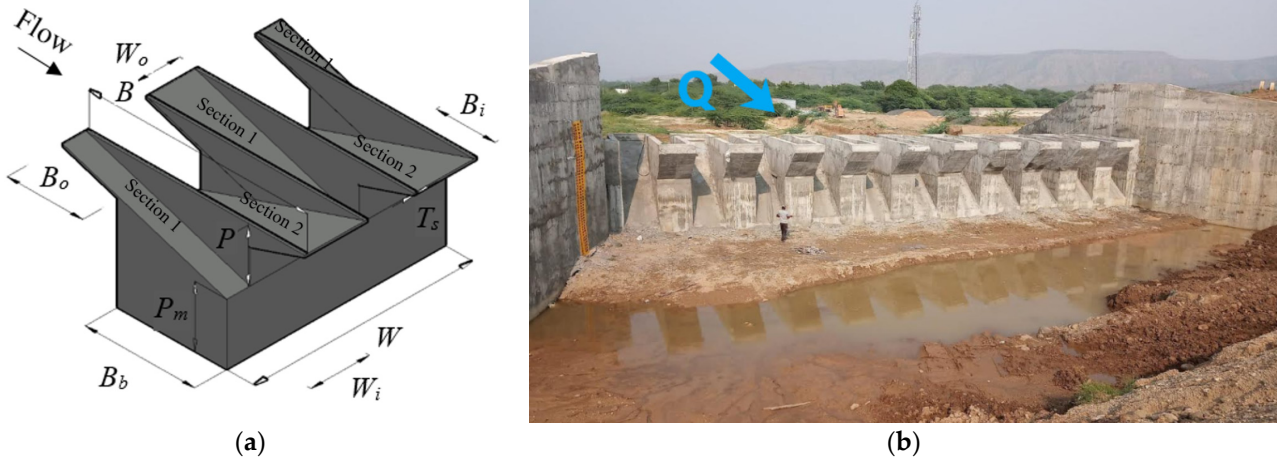
Figure 1. (**a**) Fundamental parameters of type A PK weir -3D view. (**b**) Piano key weir for storage reservoir near Thimmapuram and Gaddamvaripalli village, Andhra Pradesh, India.
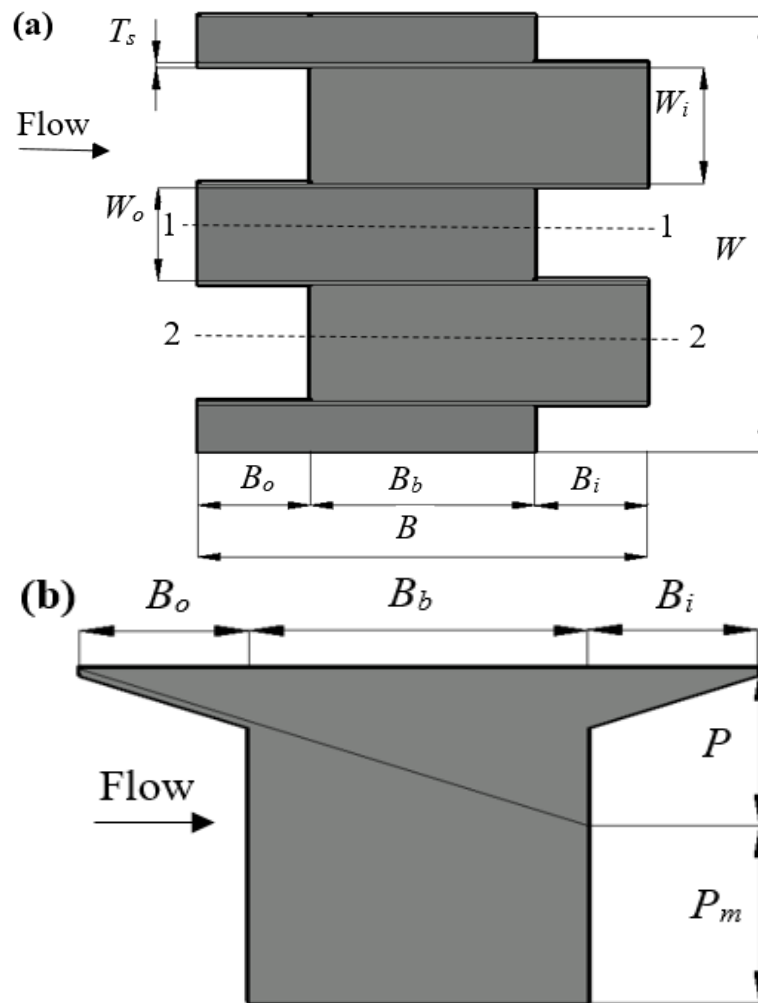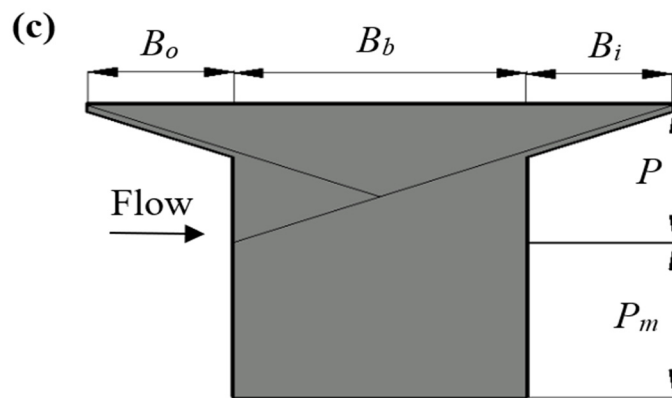

Figure 2. *Cont.*

Figure 2. (**a**) Top view of PK weir type A model, (**b**) Side view of PK weir at Section 1, (**c**) Side view of PK weir at Section 2 [20].

Figure 3. Types of PK weirs (A, B, C, and D).

Recently developed numerical and CFD techniques can predict the discharge capacity of the PK weir [21]. Several equations are available to calculate the discharge coefficient under free-flow conditions and even fewer for submerged flow conditions. Crookston et al. [9,21] conducted an experimental study on PK weir and proposed an equation for the discharge coefficient. Using computational fluid dynamics (CFD) models, the head and discharge relation was calculated, and it was concluded that CFD models are good for estimating the experimental results. Khassaf et al. [22] conducted an experimental study on fourteen physical models under submerged conditions and proposed an equation for the discharge coefficient, PK weir layout, and sloping floors with overhangs keys upstream and downstream to reduce the footprint area.

Pralong et al. [23] provided standard geometrical parameters of PK weir. Cicero and Delisle [24] studied the discharge characteristics of PK weirs type A, type B, and type C and concluded that type B PK weir gives more discharge than type A and type

C PK weir. Definitions of parameters given by investigators for PK weir type A are in Table 1. Seyedjavad et al. [25] investigated the discharge capacity of trapezoidal PK side weir and labyrinth side weir. The author concluded that the trapezoidal PK side weir discharge coefficient is 1.2, and 1.87 times the trapezoidal labyrinth side weir with 12° and 6°, respectively, and 1.5 times the triangular labyrinth side weir. The trapezoidal PK side weir was given the highest CD for $0.2 < H/P < 0.4$. Ghanbari and Heidarnejad [26] investigated a triangular notch's effect on the PK weir's discharge capacity. The author used FLOW 3D software to study flow hydraulics and concluded that CD of a triangular PK weir is 25% higher than the rectangular PK weir and by changing the notch shape of PK weir, increased the CD of PK weir by 36% and 13% for the heights of 5 cm and 7.5 cm, respectively.

Al-Baghdadi and Khassaf [27] proposed an empirical equation for calculating the value of CD, and it depends on dimensionless ratios of L/W and H/P. Al-Shukur et al. [28] conducted an experimental study to check the influence of piano key weir geometry on CD. They proposed an empirical relation to calculate the C_D for type B PK weir at Pi/Po = 0.7 using experimental data and concluded that discharge capacity increases by 42% with the increase in L/W and P_i/P_o. Eslinger and Crookston [29] investigated energy dissipation of type A PK weir by changing the ratio of W_i/W_o at various H/P ratios and concluded that the energy dissipation rate is high in low flows and low in high flows. Li et al. [20] investigated the effect of auxiliary geometrical parameters on the discharge capacity of the piano key weir. They concluded that by adding the auxiliary geometrical parameters, the author observed an increase in CD of 16.8% compared to without auxiliary geometric parameters and proposed an equation for CD. Khassaf and Al-Baghdadi [30] investigated the effect of sidewall angle and sidewall inclination angle on CD and concluded that by increasing the sidewall angle from 0° to 5°, discharge capacity increases by 4%. However, an increment in the sidewall angle greater than 10° decreases the discharge capacity by 18%. Kumar et al. [31] conducted an experimental study on trapezoidal and rectangular PK weir and concluded that trapezoidal PK weir gives 2–15% more discharge than rectangular PK weir.

This paper summarizes the current state of the knowledge about PK weir hydraulics to provide a comprehensive overview and a reference list to students, researchers, and practitioners, allowing them to better understand how such a complex structure works as well as future research and development steps.

2. Geometrical Parameters of PK Weir

The PK weir's geometrical parameters are L, the total developed length of the crest axis, P, PK weir height, and some more parameters are given in Table 1. Due to the nonlinear overflow structure, it shows a complex flow pattern. The PK weir can allow the flow up to 100 (m³/s/m) specific discharge [1–6]. The physical models of labyrinth weir and PK weir are required to check hydraulic performance for low and high flow heads [1]. The geometrical parameters and their definitions of the piano key weir are shown in Figure 1a and Table 1. Figure 1b shows a filed picture of recently constructed piano key wire for storage reservoir near Thimmapuram and Gaddamvaripalli village, Andhra Pradesh, India.

Figure 2 illustrates the cross-section and plan view of the PK weir. The efficiency of PK weirs decreases with an increase in the upstream head [17,19]. Pralong et al. [23] stated that L/W and W_i/W_o ratios are the most influential parameters for calculating the PK weir discharge capacity, while B_o/B_i ratio is the least influential parameter. The value of C_D increases with an increase in the L/W ratio [23] and the B/P ratio [18], while Machiels et al. [19] found that the P/W ratio is more effective than the B/P and the W_i/W_o ratios. For high and low flows, the optimum ratio of P/W is 1.3 and 0.5, respectively [19].

3. Available Equations of C_D

Lempérière and Ouamane [1] assumed PK weir is a linear structure and gave an equation

$$Q = C_{DL} W \sqrt{2gH^3} \tag{1}$$

C_{DL} = Discharge coefficient of a linear weir, W = Linear channel width, H = Head over the weir crest on the upstream side of the weir. Most prototypes are designed at $H/P = 0.3$ [17], where P = Height of the PK weir.

Kabiri-Samani and Javaheri [18] conducted an experimental study on scaled physical model PK weirs types A, B, and C under a specific discharge range of 0.025 to 0.175 (m^3/s). The authors proposed a free and submerged flow equation over a sharp-crested PK weir.

$$Q_P = \frac{2}{3} C_D W \sqrt{2gH^3} \tag{2}$$

where Q_P is the discharge over PK weir, C_D is the discharge coefficient of PK weir. The effect of surface tension is small for the test above the $H = 30$ (mm), so surface tension is neglected [32]. The Reynolds number is neglected because the effect of viscosity is significantly less in the turbulent flow. By applying dimensional analysis, the equation (given by Equation (3)) with the least error and the highest $R^2 = 0.98$.

$$C_D = 0.212 \left(\frac{H}{P} \right)^{-0.675} \left(\frac{L}{W} \right)^{0.377} \left(\frac{W_i}{W_O} \right)^{0.426} \left(\frac{B}{P} \right)^{0.306} e^{1.504\left(\frac{B_o}{B} \right) + 0.093\left(\frac{B_i}{B} \right)} + 0.606 \tag{3}$$

Given parameter ranges are $0.1 \leq H/P \leq 0.6$, $2.5 \leq L/W \leq 7$, $1 \leq B/P \leq 2.5$, $0.33 \leq W_i/W_o \leq 1.22$, $0 \leq B_i/B \leq 0.26$, $0 \leq B_o/B \leq 0.26$. Free flow over a PK weir is shown in Figure 4.
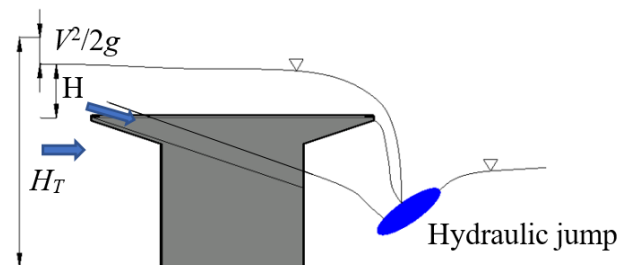

Figure 4. PK weirs under the free-flow condition.

By applying dimensional analysis, the equation of submerged flow C_s with $R^2 = 0.97$ is given by Equation (4).

$$C_s = \left\{ 1 - 0.858 \left(\frac{H_D}{H} \right) + 2.628 \left(\frac{H_D}{H} \right)^2 - 2.489 \left(\frac{H_D}{H} \right)^3 \right\} \left(\frac{L}{W} \right)^{0.055} \tag{4}$$

where C_s is the discharge coefficient for submerged flow. The ranges of parameters are $2.5 \leq L/W \leq 6$, $H_D/H > 0.6$ (H_D is head over the weir crest on the downstream side) remaining ranges are the same as free flow. The study concluded that the discharge capacity increases with the increase in inlet key width. By reducing the outlet key's width, the upstream key's local submergence increases and discharge decreases. Discharge also increases with an increase in the upstream overhang due to an increase in inlet flow area and wetted perimeter. Under the submerged flow conditions, discharge decreases with an increase in the downstream head. The author also highlighted that the proposed discharge coefficient equations for free flow and submerged flow apply to all PK weir types: type A, type B, type C, and type D.

Anderson and Tullis [16] investigated PK weir and labyrinth weirs with and without slopes. They studied hydraulic behaviour on different weirs, which they categorized in different forms, such as the PKL, RLRIO, RLRI, RLRO, and RL. The PKL model is the piano key weir with both side overhangs, the RLRIO model is a rectangular labyrinth weir with a sloped floor in both inlet and outlet key, the RLRI model is a rectangular labyrinth weir with a sloped floor in the inlet key, the RLRO model is a rectangular labyrinth weir with a sloped floor in the outlet key, and the RL model is a rectangular labyrinth weir without a sloped floor. The authors concluded that the PKL weir shows the highest discharge efficiency compared to others except the RL weir within the range of $H/P < 0.15$ (H is the water head on the crest of the weir). Crookston et al. [2] proposed a C_D equation given in Equation (5) for the Anderson and Tullis [16] experimental study data.

$$C_D = \left[\frac{1}{a_1 + b_1\left(\frac{H}{P}\right) + \frac{c_1}{\left(\frac{H}{P}\right)}} + d_1\right]\left(\frac{L}{W}\right) \tag{5}$$

where a_1, b_1, c_1, and d_1 are constants given by the author for the different inlet to outlet key ratios. For the $W_i/W_o = 1$, a_1, b_1, c_1 and d_1 are 0.5091, 10.29, 0.09712 and 0.1164 respectively.

Ribeiro et al. [17] conducted an experimental study on type A PK weir with the free flow condition. Specific discharges ranged between 0.026 to 0.440 (m³/s) and applied to PK weirs with a half circular rounded crest. Taylor [33] introduced the discharge enhancement ratio (r) compared between the sharp-crested linear and labyrinth weirs. The labyrinth weir has a flat base area that is not suitable for the dam's crest. The piano key weir has less footprint area and a well-balanced, safe, and economic structure. The hydraulic behaviour of the PK weir is different from the labyrinth weir. Design procedures are different for both labyrinth and PK weir, and detailed design and construction matters are given by Laugier [15]. Discharge enhancement ratio (r) is the ratio of PK weir discharge to linear weir discharge and is calculated as Equations (6a)–(6d).

$$r = \frac{Q_P}{Q} = \frac{Q_P}{0.42W\sqrt{2gH^3}} \tag{6a}$$

$$C_D = 0.63 * r \tag{6b}$$

$$r = 1 + 0.24\left(\frac{(L-W)P_i}{WH}\right)^{0.9}(WPW_iW_o) \tag{6c}$$

$$W = \left(\frac{W_i}{W_o}\right)^{0.05} \text{ and } P = \left(\frac{P_i}{P_o}\right)^{0.25} \tag{6d}$$

where P_i is inlet key weir height, P_o is outlet key weir height.

The authors concluded that PK weir discharge efficiency increases for low heads, and its efficiency decrease rapidly by increasing head overflow above the weir crest. Flow behaviour is different from the labyrinth weir and flows divided into two parts; one from the inlet overflows as a thin screen, and another from the outlet flows similar to a jet at the bottom. According to the updated design flood requirement, the additional release capacity is improved by constructing the PK weir with the previous spillway system. High-velocity flows can create cavitation, cracks, development of turbulence, and uplift pressure to reduce the existing system's safety. It is recommended that old dams with inferior surface characteristics provide some thickness slab for downstream protection [2,15]. The PK weir stabilization is done by adding a counterweight on the upstream side. The dam's internal stability depends on the material used to construct the PK weir.

Cicero and Delisle [24] conducted an experimental study on the discharge characteristics of piano key weir under submerged flow. The authors tested the efficiency of PK weir

types A, B, and C to isolate the overhang effect on both free and submerged flow conditions. The authors proposed Equation (7) to calculate the discharge coefficient.

$$C_D = \frac{3}{2}\left[a_2 + a_3\left(\frac{H}{P}\right) + a_4\left(\frac{H}{P}\right)^2 + a_5\left(\frac{H}{P}\right)^3 + a_6\left(\frac{H}{P}\right)^4\right] \tag{7}$$

where a_2, a_3, a_4, a_5, and a_6 are coefficients of Equation (7). For type A PK weir, ranges of parameters and coefficients are $0.1 < H/P < 0.72$ and $a_2 = 1.63$, $a_3 = 0.59$, $a_4 = -11.56$, $a_5 = 21.72$ and $a_6 = -12.46$; For type B PK weir, ranges of parameters and coefficients are $0.1 < H/P < 0.71$, and $a_2 = 1.54$, $a_3 = 3.27$, $a_4 = -22.15$, $a_5 = 37.32$ and $a_6 = -20.37$. For type C PK weir, ranges of parameters and coefficients are $0.1 < H/P < 0.79$, and $a_2 = 1.91$, $a_3 = -3.85$, $a_4 = 4.17$, $a_5 = -1.56$ and $a_6 = 0$. Comparing the C_D for type A, B, and C PK weirs at 0.1 to 0.9 of H/P showed that the type B PK weir is 10% more efficient than the type A and the type C.

Under submerged flow conditions, type A PK weir was 40%, 50–70%, and 50–60% more efficient than the ogee crested weir, sharp-crested weir, and broad crested weir [24], respectively. Thus, type B and type C are more efficient than linear weirs. For $s > 0.7$, the broad crested weir is more efficient than the sharp-crested weir [24]. Figure 5 illustrates the PK weir under submerged flow conditions. Tullis et al. [34] concluded that sensitivity for submergence is type B > type A > type C. The PK weir is more sensitive for submergence with a long broad crested weir and less sensitive for the sharp-crested weir [24,34–36].
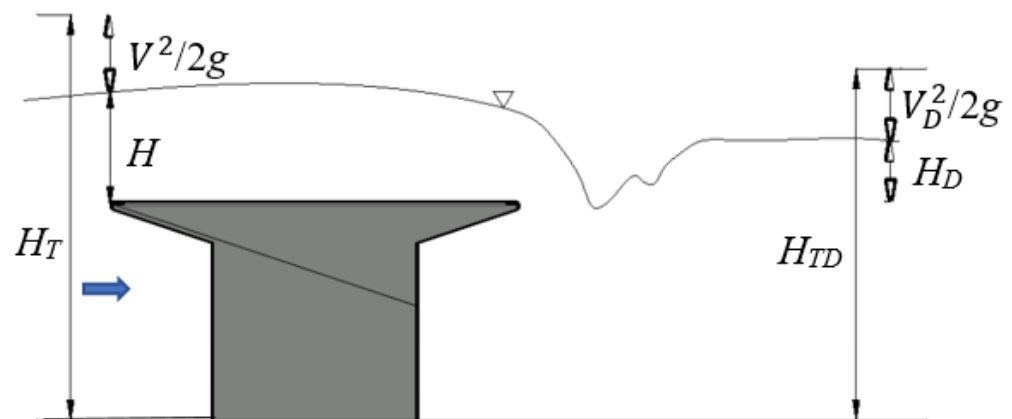

Figure 5. PK weir under submerged condition, where V and V_D are the upstream and downstream velocity of the PK weir.

Al-Baghdadi and Khassaf [27] investigated the crest length effect on the discharge capacity of PK weirs. The author conducted experiments for five physical models with $L/W = 3, 4, 5, 6,$ and 7, with constant values of $W_i/W_o = 1.25$, $B/P = 2.4$, $B_i/B = 0.25$, $B_o/B = 0.25$. Using their experimental outcomes, the authors proposed Equation (8) for calculating the C_D.

$$C_D = a_7\left(\frac{H}{P}\right)^{a_8} \tag{8}$$

where a_7 and a_8 are the constants, and the values of these constants are given in Table 2. The authors found that C_D decreases by increasing the H/P ratio. For lower values of L/W, the authors found that the value of C_D is also lowered. The author proposed one more empirical equation, i.e., Equation (9) for $3 \leq L/W \leq 7$ and $0.15 \leq H/P \leq 1.95$.

$$C_D = 0.6793\left(\frac{H}{P}\right)^{-0.4421}\left(\frac{L}{W}\right)^{0.4354} \tag{9}$$

Table 2. Values of coefficients a and b for different L/W ratios.

L/W	a_7	a_8	R^2
3	1.1197	−0.300	0.9908
4	1.2566	−0.433	0.9982
5	1.3042	−0.479	0.9986
6	1.4088	−0.496	0.9972
7	1.5263	−0.469	0.9883

Comparison between predicted and observed values of C_D found within the range of $\pm 10\%$ errors, and the authors concluded that the discharge coefficient (C_D) consequently changes with *L/W* for a given head. Furthermore, the authors showed that an increase in the *L/W* ratio always benefits C_D, as shown in Figure 6.
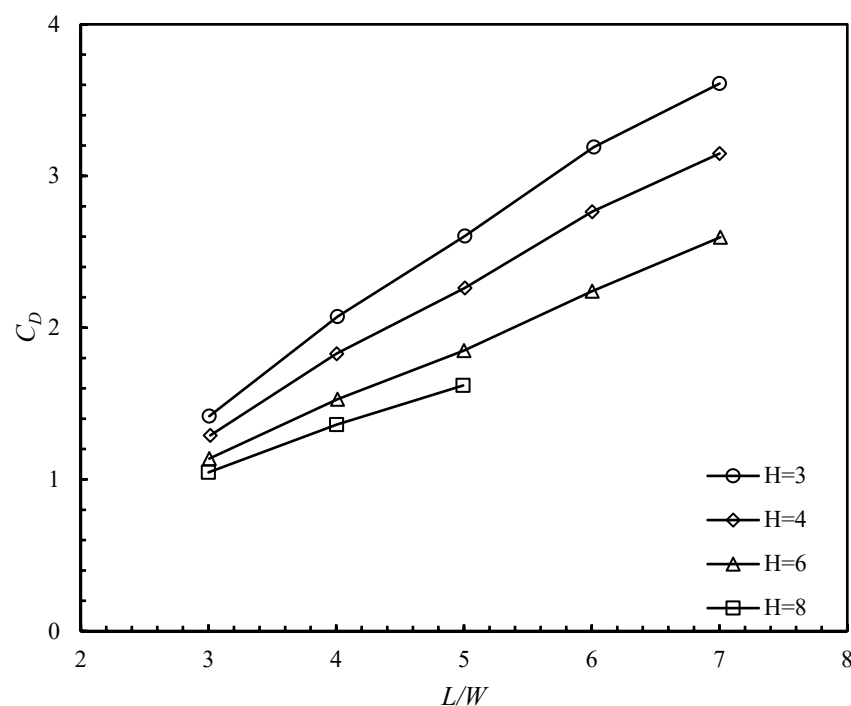

Figure 6. Variation of C_D with *L/W* ratio.

Al-Shukur and Al-Khafaji [28] experimentally investigated the effects of type B PK weir geometry on discharge efficiency. The authors proposed optimum design criteria and provided the best outlet slope, where PK weir acts as an energy dissipation structure by forming a hydraulic jump. The authors proposed Equation (10) for calculating the value of C_D given as

$$C_D = 0.8816 \left[\frac{H}{P}\right]^{-0.8539} \left[\frac{L}{W}\right]^{0.3619} \left[\frac{W_i}{W_o}\right]^{0.0802} e^{\left(0.0527\left(\frac{B}{P}\right) - 1.2182\left(\frac{P_i}{P_o}\right)\right)} + 0.5346 \quad (10)$$

This equation is only valid for limited values of *L/W*, W_i/W_o, *B/P*, and P_i/P_o viz. $3 \leq L/W \leq 7$, $0.5 \leq W_i/W_o \leq 2$, $1.5 \leq B/P \leq 5$, and $0.7 \leq P_i/P_o \leq 2$. The authors stated that the P_i/P_o ratio significantly influences discharge capacity through PK weirs. For $P_i/P_o > 1$, the dimensions do not meet PK weir standards because of the scale effect, but for $P_i/P_o \leq 1$, the authors observed a significant effect on the PK weir discharge capacity. A P_i/P_o ratio less than 0.7 could not be explored since its production was beyond the capabilities of the piano key weir. According to the laboratory experiments, the ideal value of the P_i/P_o ratio was 0.7, as shown in Figure 7.
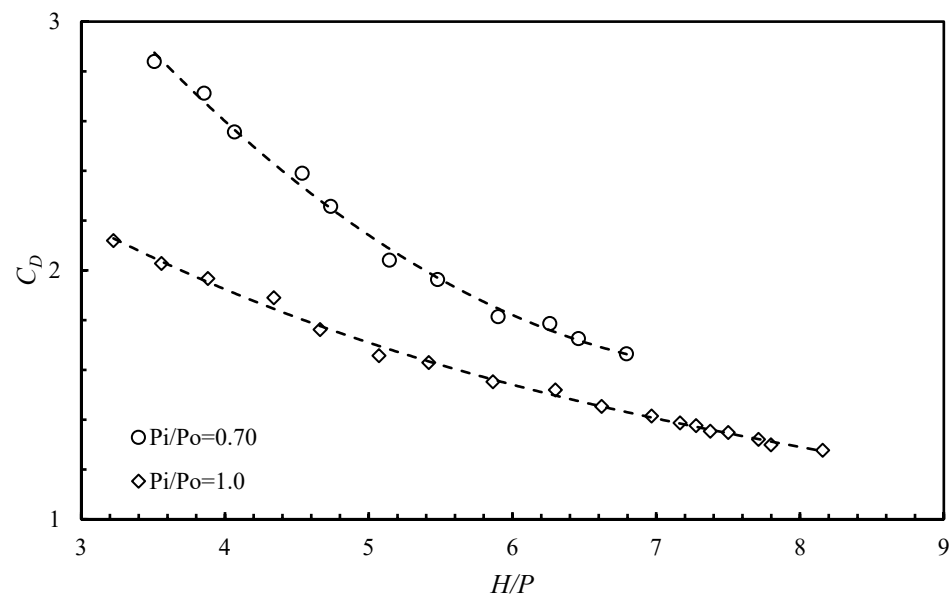
Figure 7. Variation of C_D with H/P.

Li et al. [20] conducted an experimental study on type A PK weir with auxiliary geometries, such as nose and parapet wall. The author prepared six physical models. They are the M_A model (PK weir without triangular nose, rounded nose, and parapet wall), the M_{AT} model (PK weir with triangular nose), the M_{AR} model (PK weir with rounded nose), the M_{AP16} model (PK weir with 16 (mm) parapet wall on weir crest), the M_{AP25} model (PK weir with 25 (mm) parapet wall on weir crest), and the M_{ARP25} model (PK weir with rounded nose and 25 (mm) parapet wall on weir crest). By using experimental results on PK weir, the author proposed the C_D equation given in Equation (11).

$$C_D = \left[a_9 + a_{10}\left(\frac{H}{P}\right) + a_{11}\left(\frac{H}{P}\right)^2 + a_{12}\left(\frac{H}{P}\right)^3 + a_{13}\left(\frac{H}{P}\right)^4 \right] \tag{11}$$

where a_9, a_{10}, a_{11}, a_{12}, and a_{13} are the coefficients of corresponding fitting formula values shown in Table 3. The author concluded that the M_{AT} and M_{AR} models gave similar results and the discharge capacity of the M_{AT} and M_{AR} models is greater than the M_A model. The author observed that the influence of auxiliary geometric parameters is more when the water head over the weir crest is low. The model M_{AP16} gave 1% more discharge capacity than the M_{AP25} model for low water head over the weir crest. The author observed that the M_{AP25} model gave more discharge for the high-water heads than the M_{AP16} model because nappe formation is more for the M_{AP25} model. The model M_{ARP25} is given 11.6–16.8% more discharge capacity than the M_A model. The discharge coefficient was greatly enhanced by adding parapet walls, which increased the PK weir discharge capacity, as shown in Figure 8.

Table 3. Coefficients of corresponding fitting formulas.

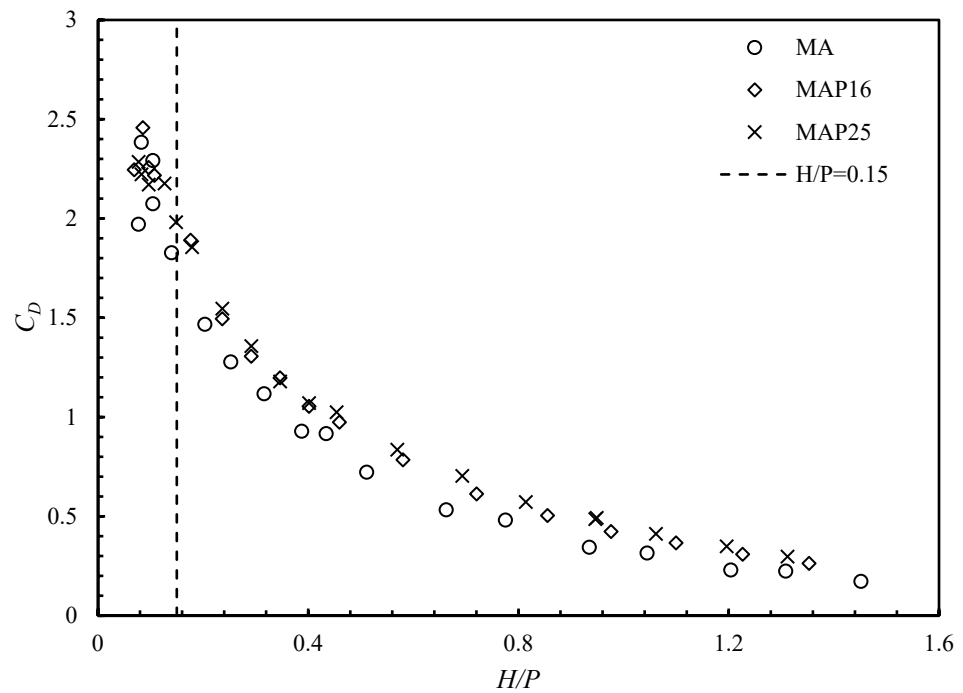| a_9	a_{10}	a_{11}	a_{12}	a_{13}	H/P	R^2
2.4	−4.31	4.64	−2.46	0.51	0.15–1.46	0.998

Figure 8. Variation of C_D with H/P ratio for models M_A, M_{AP16}, and M_{AP25}.

Guo et al. [36] investigated the previous experimental studies to propose the C_D equation based on the experimental data. The experimental studies of Ribeiro et al. [17] and Kabiri-Samani and Javaheri [18], and Machiels et al. [19] are considered, and observed data sets are taken within the geometrical parameters ranges of $H/P > 0.1$, $2.5 < L/W < 8.5$, $0 < W_i/W_o < 2.45$, $1 < B/P < 6$, these geometric ranges fall within the author's proposed ranges of parameters. The author analyzed 18 experimental data of type A PK weir for deriving Equation (12).

$$C_D = 0.285 \left[\frac{H}{P}\right]^{-0.465} \left[\frac{L}{W}\right]^{0.45} \left[\frac{W_i}{W_o}\right]^{0.05} \left[\frac{B}{P}\right]^{0.1} + 0.1 \tag{12}$$

The predicted values of the discharge coefficient have an average error of $\pm 10\%$ for low and high heads and the least error for medium heads ratios, i.e., $< \pm 5\%$.

Kumar et al. [31] conducted experiments on PK weirs with rectangular and trapezoidal configurations. The author used soft computing techniques viz. M_5 and random forest techniques to estimate the discharge coefficient. The applied geometric parameters were identical for both weirs. The author found that the gain in discharge for a trapezoidal weir was more than a rectangular weir. The author proposed the discharge coefficient equation for different values of H/P and L/W.

For rectangular PK weirs:

$H/P \leq 0.249$ and $L/W \leq 5.5$ $\qquad C_D = -4.0038\, H/P + 0.338\, L/W + 0.569 \tag{13}$

$H/P \leq 0.249$ and $L/W > 5.5$ $\qquad C_D = -5.1737\, H/P + 0.285\, L/W + 1.185 \tag{14}$

$H/P > 0.249$ $\qquad C_D = -2.4112\, H/P + 0.1944\, L/W + 1.03 \tag{15}$

For trapezoidal PK weirs:

$H/P \leq 0.249$ and $L/W \leq 5.5$ $\qquad C_D = -4.8713\, H/P + 0.3707\, L/W + 0.653 \tag{16}$

$H/P \leq 0.249$ and $L/W > 5.5$ $\qquad C_D = -6.3375\, H/P + 0.3114\, L/W + 1.368 \tag{17}$

$$H/P > 0.249 \qquad\qquad C_D = -2.7319\,H/P + 0.193\,L/W + 1.98 \qquad\qquad (18)$$

Discharge coefficients gain in the trapezoidal PK weir was 2–15% more than in the rectangular PK weir. After performing the statistical analysis, the author observed that the random forest regression approach performed better than M_5.

Figure 9 illustrates the variation between discharge enhancement ratio (r) and H/P ratio. Kumar et al. [31] observed that the values of r are higher for the TPK weirs than the RPK weirs. The author found that an increase in the L/W ratio significantly increased the discharge capacity of both types of PK weirs, as seen in Figure 9.
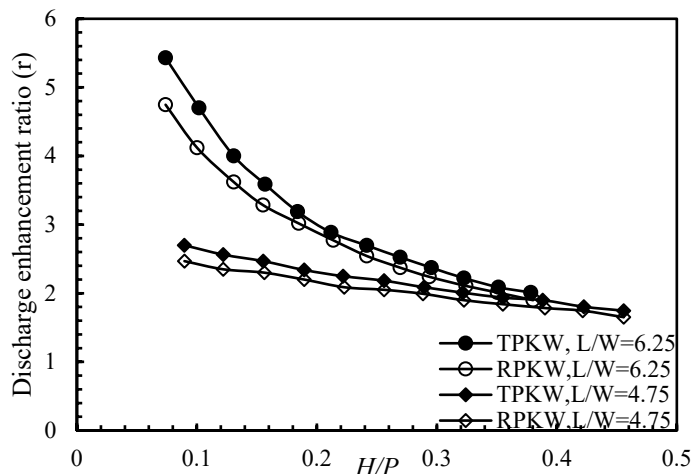

Figure 9. Variation of r with H/P ratio; TPKW: Trapezoidal piano key weirs and RPKW: Rectangular piano key weirs.

Singhal et al. [37] conducted an experimental study to know the effect of inlet key width to outlet key width ratio, L/W ratio, and sloped floors on the discharge capacity of type A PK weir. A total of 18 models were tested in three sets, each containing six models. The first set of six model dimensions are given in Table 4; these first set of models are without a sloped floor. The second set of six models is with a sloped floor and the exact dimensions as the first set of six models. Finally, the third set of six model dimensions is given in Table 5, and the third set of models is with a sloped floor. The author concluded that increasing the L/W ratio increases the discharge capacity of a piano key weir. Sloped floor models are given high discharge, and the author observed that the model with a W_i/W_o ratio of one is giving more discharge; an L/W ratio does not show any change in the discharge capacity of PK weir at an H/P ratio that is more than 0.6. The author proposed a C_D equation for different L/W ratios as given in Equations (19)–(21).

$$\text{For } L/W = 3.56 \quad C_D = 0.6858\left(\frac{H}{P}\right)^{-0.305} \qquad\qquad (19)$$

$$\text{For } L/W = 4.84 \quad C_D = 0.667\left(\frac{H}{P}\right)^{-0.3703} \qquad\qquad (20)$$

$$\text{For } L/W = 7.4 \quad C_D = 0.688\left(\frac{H}{P}\right)^{-0.4673} \qquad\qquad (21)$$

Table 4. First set of dimensions for the six models.

Model	W_i (cm)	W_o (cm)	L/W	Weir Height (cm)
M_{11}	5	5	7.40	12
M_{12}	5	5	7.40	16
M_{13}	5	5	7.40	20
M_{14}	12.5	12.5	3.56	12
M_{15}	12.5	12.5	3.56	16
M_{16}	12.5	12.5	3.56	20

Table 5. Third set of dimensions for the six models.

Model	W_i (cm)	W_o (cm)	L/W	Weir Height (cm)
M_{31}	6.00	4.00	7.40	16
M_{32}	4.00	6.00	7.40	16
M_{33}	10.00	6.67	4.84	16
M_{34}	6.67	10.00	4.84	16
M_{35}	8.33	8.33	4.84	16
M_{36}	10.00	15.00	3.56	16

Khassaf and Al-Baghdadi [30] investigated an experimental study on the PK weir with a change in sidewall angle (α) and sidewall inclination angle (β). A total of five models were investigated, the first model (M) without change in α and β, second model ($\alpha5$) with $\alpha = 5°$ and $\beta = 0°$, third model ($\alpha10$) with $\alpha = 10.25°$ and $\beta = 0°$, fourth model ($\beta5$) with $\alpha = 0°$ and $\beta = 5°$, and fifth model ($\beta10$) with $\alpha = 0°$ and $\beta = 10°$. From the reported results, the second model ($\alpha5$) discharge capacity is 4% higher than the first model (M); the third model ($\alpha10$) discharge capacity is 5.5–8% lower than the first model (M), as shown in Figure 10; fourth model ($\beta5$) and fifth model ($\beta10$) discharge capacity is 2.5% and 18% less than the first model (M), respectively. The author concluded that sidewall angle (α) ranges between 0°–5° gave the positive results and more than a 5° gave the negative effect on discharge capacity, and the author proposed a C_D equation to estimate the discharge capacity given in Equation (22) and coefficients of equation a_{14} and a_{15}, which are given in Table 6.

$$C_D = a_{14} \left(\frac{H}{P} \right)^{a_{15}} \tag{22}$$

Table 6. The coefficients of equation (22) for the various models.

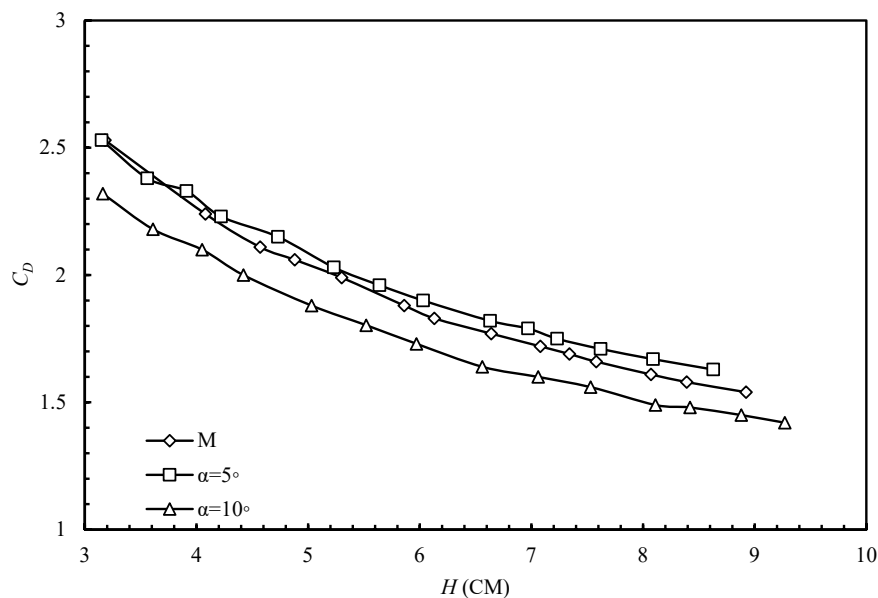| Model	a_{14}	a_{15}	H/P	R^2
M	1.3042	−0.479	0.25–0.71	0.9986
$\alpha5$	1.3161	−0.448	0.23–0.63	0.9975
$\alpha10$	1.1432	−0.458	0.21–0.62	0.9972
$\beta5$	1.3009	−0.499	0.25–0.71	0.9937
$\beta10$	1.2213	−0.384	0.25–0.78	0.9768

Figure 10. Variation of C_D with H.

4. Sensitivity Analysis

In this study a sensitivity analysis is carried out by us to obtain the most effective dimensionless parameter in the C_D equation. The Kabiri-Samani and Javaheri [18] proposed C_D equation is selected for sensitivity analysis because the proposed equation has maximum geometric dimensionless parameters. This study assumes that errors are independent for each input parameter [38–45]. X is the input, and those that are H/P, L/W, W_i/W_o, B/P, B_o/B, B_i/B, and Y are the CD output. The inputs values are $H/P = 0.5$, $L/W = 5$, $W_i/W_o = 1$, $B/P = 2.5$, $B_o/B = 0.16$, $B_i/B = 0.1$ (Note that the values of dimensionless geometric parameters are taken from the author proposed ranges). ΔX is the 10% increment and decrease in input X. Y_X is the Y output at X input, and $Y_{X+\Delta X}$ is Y output at $X + \Delta X$ input. ΔY is the difference between Y_X and $Y_{X+\Delta X}$. The absolute sensitivity (AS) is calculated as AS $= \Delta Y / \Delta X$, and the relative error is RE $= \Delta Y / Y$. The relative sensitivity is RS $= X\Delta Y / Y\Delta X$ [39,40]. From Table 7, at X input $H/P = 0.5$, $L/W = 5$, $W_i/W_o = 1$, $B/P = 2.5$, $B_o/B = 0.16$, $B_i/B = 0.1$, the output C_D (Y_X) is 1.839, with 10% increment in X that is $X + \Delta X = 0.5 + 0.05$ in H/P and with the no change in remaining inputs, the output C_D ($Y_{X+\Delta X}$) is 1.762, similar to the 10% decrease in X, given in Table 8. The sensitivity analysis results show that the L/W ratio is the most sensitive parameter in the C_D equation, followed by the B/P ratio. The RS is more for the L/W input ratio, followed by B/P, W_i/W_o, H/P, B_o/B, and B_i/B for both 10% increment and decrease in the input ratios shown in Tables 7 and 8.

Table 7. Sensitivity and error analysis (X is an input parameter, ΔX is a 10% increase in X, and ΔY is a change in the output (C_D).

Input (X)	ΔX	$Y_{X+\Delta X}$	ΔY	AS	RE	RS
H/P	0.05	1.762	−0.076	−1.537	−0.041	−0.001
L/W	0.5	1.884	0.045	0.090	0.024	0.061
W_i/W_o	0.1	1.890	0.051	0.511	0.027	0.002
B/P	0.25	1.875	0.036	0.146	0.019	0.012
B_o/B	0.016	1.869	0.030	1.877	0.016	4.18×10^{-5}
B_i/B	0.01	1.840	0.001	0.114	0.0006	6.2×10^{-7}

Table 8. Sensitivity and error analysis (X is an input parameter, ΔX is a 10% decrease in X, and ΔY is a change in the output (C_D).

Input (X)	ΔX	$Y_{X-\Delta X}$	ΔY	AS	RE	RS
H/P	0.05	1.930	0.090	1.818	0.049	0.001
L/W	0.5	1.791	−0.048	−0.096	−0.026	−0.065
W_i/W_o	0.1	1.785	−0.054	−0.541	−0.029	−0.003
B/P	0.25	1.800	−0.039	−0.156	−0.021	−0.013
B_o/B	0.016	1.810	−0.029	−1.832	−0.016	-4.08×10^{-5}
B_i/B	0.01	1.838	−0.001	−0.114	−0.0006	-6.2×10^{-7}

5. Future Research and Next Developments Stages

Till now, studies are available on different configurations of PKW to understand the various performances of the weir, but some areas are left out while conducting the experiments. This includes arrangements of different shapes and types of the weir, i.e., some works have been done only for type A, while others conducted with type B only, different dimensions of the weir, discharge rate, shape, and size of sediment, etc. For scouring at PKW, limited research work is available. Hence, it is essential to conduct studies for analyzing the scour studies around PKW. For energy dissipation, it is found that most of the experiments are conducted using Type A PKW only. So, it has been recommended that some other geometries, such as types B, C, and D of PKW, should be considered while conducting experiments in the future, along with energy dissipation scale effect studies for field-scale PKW.

6. Conclusions

Different authors have investigated the ways and designs of PK weirs to increase their discharge capacity. Previous studies on PK weirs demonstrate that the PK weir's discharge capacity increased by increasing the inlet key width, upstream overhang, and sloped floors to the inlet key and outlet key. PK weir type B is 10% more efficient than type A and type C. The increase in L/W ratio shows an increase in the C_D of the PK weir, and it is observed that an 11.6–16.8% increase in C_D by adding the auxiliary geometric parameters to the PK weir and the trapezoidal PK weir C_D is 2–15% more than the rectangular PK weir. Furthermore, a 4% increase and an 8% decrease in the C_D by increasing the sidewall angle from 0° to 5° and 10° was observed. From sensitivity analysis, it is observed that the Kabiri-Samani and Javaheri [18] proposed C_D equation is more sensitive for the L/W dimensionless ratio. The relative sensitivity is more for the L/W ratio, followed by B/P, W_i/W_o, H/P, B_o/B, and B_i/B for both a 10% increase and decrease in the input ratios.

Author Contributions: R.K.B. collected experimental data; R.K.B. prepared the first draft; M.P. and R.K.B. analyzed the data; R.K.B. applied the methodology; M.V., M.P. and P.M. revised and edited the manuscript; and M.V. acquired funding. All authors have read and agreed to the published version of the manuscript.

Institutional Review Board Statement: Not applicable.

Informed Consent Statement: Not applicable.

Data Availability Statement: All applied data are available in the manuscript.

Conflicts of Interest: The authors declare no conflict of interest.

Notation

B = Total width of PK weir (m)
B_b = Width of the in-between portion of the inlet and outlet key (m)
B_i = Width of inlet key (m)
B_o = Width of outlet key (m)
C_{DL} = Discharge coefficient of linear weir (-)
C_D = Discharge coefficient of PK weir (-)
C_S = Submerged flow discharge coefficient (-)
H = Head over the weir crest on the upstream side of the weir (m)
H_{TD} = Total downstream head (m)
H_T = Total upstream head (m)
L = Total length of the weir crest (m)
P = Height of the weir (m)
P_m = Height of dam (m)
q = Unit discharge through a PK weir (m^3/s/m)
Q_P = Discharge over a PK weir (m^3/s)
Q = Discharge over a linear weir (m^3/s)
r = Discharge enhancement ratio (-)
V = Velocity of fluid on the upstream side of the weir (m/s)
V_D = Velocity of fluid on the downstream side of the weir (m/s)
S = Submergence ratio (-)
S_i = Inlet key slope (degrees)
S_m = Modular submergence ratio (-)
S_o = Outlet key slope (degrees)
T = Wall thickness (m)
W = Width of the weir (m)
W_i = Width of the inlet key (m)
W_o = Width of the outlet key (m)
P_i = Height of the weir at the inlet key
P_o = Height of the weir at outlet key
α = Angle between inlet/outlet key crest and side weir of PK weir (degrees)
ρ = Water density (kg/m^3)
σ = Surface tension (N/m^3)
ν = Kinematic viscosity (m^2/s)
μ = Dynamic viscosity (pa s)

References

1. Lempérière, F.; Ouamane, A. The Piano Keys weir: A new cost-effective solution for spillways. *Int. J. Hydropower Dams* **2003**, *10*, 144–149.
2. Crookston, B.M.; Tullis, B.P. Hydraulic design and analysis of labyrinth weirs. II: Nappe aeration, instability, and vibration. *J. Irrig. Drain. Eng.* **2013**, *139*, 371–377. [CrossRef]
3. Dabling, M.R.; Tullis, B.P.; Crookston, B.M. Staged labyrinth weir hydraulics. *J. Irrig. Drain. Eng.* **2013**, *139*, 955–960. [CrossRef]
4. Crookston, B.M.; Tullis, B.P. Labyrinth weirs: Nappe interference and local submergence. *J. Irrig. Drain. Eng.* **2012**, *138*, 757–765. [CrossRef]
5. Blanc, P.; Lempérière, F. Labyrinth spillways have a promising future. *Int. J. Hydropower Dams* **2001**, *8*, 129–131.
6. Chanson, H. Comparison of energy dissipation between nappe and skimming flow regimes on stepped chutes. *J. Hydraul. Res.* **1994**, *32*, 213–218. [CrossRef]
7. Chanson, H. *Hydraulic Design of Stepped Cascades, Channels, Weirs and Spillways*; Pergamon: Oxford, UK, 1995.
8. Anderson, R.M.; Tullis, B.P. Piano key weir hydraulics and labyrinth weir comparison. *J. Irrig. Drain. Eng.* **2013**, *139*, 246–253. [CrossRef]
9. Crookston, B.M.; Erpicum, S.; Tullis, B.P.; Laugier, F. Hydraulics of labyrinth and piano key weirs: 100 years of prototype structures, advancements, and future research needs. *J. Hydraul. Eng.* **2019**, *145*, 02519004. [CrossRef]
10. Erpicum, S.; Tullis, B.P.; Lodomez, M.; Archambeau, P.; Dewals, B.J.; Pirotton, M. Scale effects in physical piano key weirs models. *J. Hydraul. Res.* **2016**, *54*, 692–698. [CrossRef]
11. Tullis, B.P.; Crookston, B.M.; Young, N. Scale effects in free-flow nonlinear weir head-discharge relationships. *J. Hydraul. Eng.* **2020**, *146*, 04019056. [CrossRef]
12. Erpicum, S.; Laugier, F.; Boillat, J.L.; Pirotton, M.; Reverchon, B.; Schleiss, A.J. (Eds.) *Labyrinth and Piano Key Weirs*; CRC Press: London, UK, 2011.
13. Erpicum, S.; Silvestri, A.; Dewals, B.; Archambeau, P.; Pirotton, M.; Colombié, M.; Faramond, L. *Escouloubre Piano Key Weir: Prototype versus Scale Models*; Labyrinth and Piano Key Weirs II; CRC Press: London, UK, 2013; pp. 65–72.
14. Ribeiro, L.; Bieri, M.; Boillat, J.L.; Schleiss, A.J.; Singhal, G.; Sharma, N. Discharge capacity of piano key weirs. *J. Hydraul. Eng.* **2012**, *138*, 199–203. [CrossRef]
15. Laugier, F. Design and construction of the first Piano Key Weir spillway at Goulours dam. *Int. J. Hydropower Dams* **2007**, *14*, 94.

16. Anderson, R.M.; Tullis, B.P. Comparison of piano key and rectangular labyrinth weir hydraulics. *J. Hydraul. Eng.* **2012**, *138*, 358–361. [CrossRef]

17. Ribeiro, M.L.; Pfister, M.; Schleiss, A.J.; Boillat, J.L. Hydraulic design of A-type piano key weirs. *J. Hydraul. Res.* **2012**, *50*, 400–408. [CrossRef]

18. Kabiri-Samani, A.; Javaheri, A. Discharge coefficients for free and submerged flow over Piano Key weirs. *J. Hydraul. Res.* **2012**, *50*, 114–120. [CrossRef]

19. Machiels, O.; Erpicum, S.; Archambeau, P.; Dewals, B.; Pirotton, M. Parapet wall effect on piano key weir efficiency. *J. Irrig. Drain. Eng.* **2013**, *139*, 506–511. [CrossRef]

20. Li, S.; Li, G.; Jiang, D.; Ning, J. Influence of auxiliary geometric parameters on discharge capacity of piano key weirs. *Flow Meas. Instrum.* **2020**, *72*, 101719. [CrossRef]

21. Crookston, B.M.; Anderson, R.M.; Tullis, B.P. Free-flow discharge estimation method for Piano Key weir geometries. *J. Hydro-Environ. Res.* **2018**, *19*, 160–167. [CrossRef]

22. Khassaf, S.I.; Al-Baghdadi, M.B.N. Experimental investigation of submerged flow over piano key weir. *Int. J. Energy Environ.* **2018**, *9*, 249–260.

23. Pralong, J.; Montarros, F.; Blancher, B.; Laugier, F. A sensitivity analysis of Piano Key Weirs geometrical parameters based on 3D numerical modeling. *Labyrinth Piano Key Weirs–PKW* **2011**, *2011*, 133–139.

24. Cicero, G.M.; Delisle, J.R. Discharge characteristics of Piano Key weirs under submerged flow. *Labyrinth Piano Key Weirs II–PKW* **2013**, *2013*, 101–109.

25. Seyedjavad, M.; Naeeni, S.T.O.; Saneie, M. Laboratory investigation on discharge coefficient of trapezoidal piano key side weirs. *Civ. Eng. J.* **2019**, *5*, 1327–1340. [CrossRef]

26. Ghanbari, R.; Heidarnejad, M. Experimental and numerical analysis of flow hydraulics in triangular and rectangular piano key weirs. *Water Sci.* **2020**, *34*, 32–38. [CrossRef]

27. Al-Baghdadi, M.B.N.; Khassaf, S.I. Evaluation of crest length effect on piano key weir discharge coefficient. *Int. J. Energy Environ.* **2018**, *9*, 473–480.

28. Al-Shukur, A.H.K.; Al-Khafaji, G.H. Experimental study of the hydraulic performance of piano key weir. *Int. J. Energy Environ.* **2018**, *9*, 63–70.

29. Eslinger, R.K.; Crookston, B.M. Energy Dissipation of Type a Piano Key Weirs. *Water* **2020**, *12*, 1253. [CrossRef]

30. Khassaf, S.I.; Al-Baghdadi, M.B. Experimental study of non-rectangular piano key weir discharge coefficient. *Int. J. Energy Environ.* **2015**, *6*, 425.

31. Kumar, M.; Sihag, P.; Tiwari, N.K.; Ranjan, S. Experimental study and modelling discharge coefficient of trapezoidal and rectangular piano key weirs. *Appl. Water Sci.* **2020**, *10*, 1–9. [CrossRef]

32. Novák, P.; Čabelka, J. *Models in Hydraulic Engineering: Physical Principles and Design Application*; Pitman Publishing: London, UK, 1981; Volume 4.

33. Taylor, G. The Performance of Labyrinth Weirs. Ph.D. Thesis., University of Nottingham, Nottingham, UK, 1968.

34. Tullis, B.P.; Young, J.C.; Chandler, M.A. Head-discharge relationships for submerged labyrinth weirs. *J. Hydraul. Eng.* **2007**, *133*, 248–254. [CrossRef]

35. Machiels, O.; Pirotton, M.; Pierre, A.; Dewals, B.; Erpicum, S. Experimental parametric study and design of Piano Key Weirs. *J. Hydraul. Res.* **2014**, *52*, 326–335. [CrossRef]

36. Guo, X.; Liu, Z.; Wang, T.; Fu, H.; Li, J.; Xia, Q.; Guo, Y. Discharge capacity evaluation and hydraulic design of a piano key weir. *Water Supply* **2019**, *19*, 871–878. [CrossRef]

37. Singhal, G.D.; Sharma, N.; Ojha, C.S.P. Experimental study of hydraulically efficient piano key weir configuration. *ISH J. Hydraul. Eng.* **2011**, *17*, 18–33. [CrossRef]

38. Pandey, M.; Valyrakis, M.; Qi, M.; Sharma, A.; Lodhi, A.S. Experimental assessment and prediction of temporal scour depth around a spur dike. *Int. J. Sediment Res.* **2021**, *36*, 17–28. [CrossRef]

39. Sahay, R.R.; Dutta, S. Prediction of longitudinal dispersion coefficients in natural rivers using genetic algorithm. *Hydrol. Res.* **2009**, *40*, 544–552. [CrossRef]

40. Pandey, M.; Lam, W.H.; Cui, Y.; Khan, M.A.; Singh, U.K.; Ahmad, Z. Scour around spur dike in sand–gravel mixture bed. *Water* **2019**, *11*, 1417. [CrossRef]

41. Singh, U.K.; Jamei, M.; Karbasi, M.; Malik, A.; Pandey, M. Application of a modern multi-level ensemble approach for the estimation of critical shear stress in cohesive sediment mixture. *J. Hydrol.* **2022**, *607*, 127549. [CrossRef]

42. Pandey, M.; Sharma, P.K.; Ahmad, Z.; Singh, U.K. Experimental investigation of clear-water temporal scour variation around bridge pier in gravel. *Environ. Fluid Mech.* **2018**, *18*, 871–890. [CrossRef]

43. Michalis, P.; Sentenac, P. Subsurface condition assessment of critical dam infrastructure with non-invasive geophysical sensing. *Environ. Earth Sci.* **2021**, *80*, 556. [CrossRef]

44. Michalis, P.; Vintzileou, E. The Growing Infrastructure Crisis: The Challenge of Scour Risk Assessment and the Development of a New Sensing System. *Infrastructures* **2022**, *7*, 68. [CrossRef]

45. Ahmad, Z. Prediction of longitudinal dispersion coefficient using laboratory and field data: Relationship comparisons. *Hydrol. Res.* **2013**, *44*, 362–376. [CrossRef]